DIABLO Promotes Apoptosis by Removing MIHA/XIAP from Processed Caspase 9

Paul G. Ekert,*‡ John Silke,* Christine J. Hawkins,§ Anne M. Verhagen,* and David L. Vaux*

*The Walter and Eliza Hall Institute, The Royal Melbourne Hospital, Victoria 3050, Australia; ‡Murdoch Children's Research Institute and §Department of Haematology and Oncology, Royal Children's Hospital, Parkville 3052, Australia

Abstract. MIHA is an inhibitor of apoptosis protein (IAP) that can inhibit cell death by direct interaction with caspases, the effector proteases of apoptosis. DIABLO is a mammalian protein that can bind to IAPs and antagonize their antiapoptotic effect, a function analogous to that of the proapoptotic *Drosophila* molecules, Grim, Reaper, and HID. Here, we show that after UV radiation, MIHA prevented apoptosis by inhibiting caspase 9 and caspase 3 activation. Unlike Bcl-2, MIHA functioned after release of cytochrome *c* and DIABLO from the mitochondria and was able to bind to both processed caspase 9 and processed caspase 3 to prevent feedback activation of their zymogen forms. Once released into the cytosol, DIABLO bound to MIHA and disrupted its association with processed caspase 9, thereby allowing caspase 9 to activate caspase 3, resulting in apoptosis.

Key words: apoptosis • IAPs • DIABLO • caspases • BIR

Introduction

Inhibitors of apoptosis (IAPs)[1] were first identified as baculoviral genes that could suppress apoptosis of infected insect cells (Crook et al., 1993). Cellular IAP homologues such as MIHA (the human homologue is known as XIAP and hILP) (Duckett et al., 1996; Liston et al., 1996; Uren et al., 1996) have been identified that can directly bind to activated caspases (Kaiser et al., 1998; Hawkins et al., 1999; Meier et al., 2000) and inhibit apoptosis in response to a diverse range of stimuli (LaCasse et al., 1998; Uren et al., 1998). While not all IAPs have been shown to bind to caspases, all bear one or more copies of a motif termed a baculoviral IAP repeat (BIR) (Crook et al., 1993; Clem and Miller, 1994). These motifs are required for the interaction with caspases.

XIAP, which bears three BIRs, can bind to and inhibit active, processed caspase 3 with a K_i of 0.7 nM (Deveraux et al., 1997; Roy et al., 1997; Takahashi et al., 1998). Its second BIR (BIR2) and flanking regions NH_2 terminal to it have been shown to be necessary and sufficient for caspase 3 inhibition in vitro (Takahashi et al., 1998). XIAP has also been reported to bind to caspase 9 in both its zymogen and processed form (Sun et al., 2000), as well as to inhibit caspase 9 activity in vitro (Deveraux et al., 1998). However, in this case the interaction involves the COOH-terminal half of XIAP which contains BIR3 and a RING finger domain (Deveraux et al., 1999).

In both insects and mammals, proapoptotic proteins that bind directly to IAPs can antagonize IAP activity. For example, in *Drosophila*, DIAP1 is directly bound and antagonized by Grim, HID, and Reaper (Hay et al., 1995; Vucic et al., 1997, 1998; Song et al., 2000), and Grim, HID, and Reaper killing probably requires this interaction with IAPs (Wang et al., 1999; Goyal et al., 2000). These *Drosophila* proapoptotic molecules can also induce apoptosis of mammalian cells and bind to mammalian IAPs (Claveria et al., 1998; McCarthy and Dixit, 1998; Haining et al., 1999). The only mammalian protein known to bind to and antagonize the antiapoptotic effects of IAPs is DIABLO (also known as Smac) (Du et al., 2000; Verhagen et al., 2000).

To determine how DIABLO acts to promote apoptosis and how MIHA functions to inhibit it, we analyzed their interactions with each other and with caspases in NT2 cells exposed to apoptotic stimuli and in a yeast system in which the Apaf-1, caspase 9, and caspase 3 pathway had been reconstituted. To inhibit apoptosis, MIHA functioned downstream of mitochondrial release of cytochrome *c* and DIABLO. MIHA was able to inhibit caspase 9 and caspase 3 processing after UV radiation of NT2 cells and was able to bind to both processed caspase 3 and processed caspase 9, indicating it functioned mainly at the level of processed caspase 9. The pattern of caspase activation in mammalian cells and in yeast revealed that caspase 3 and caspase 9 are involved in a feedback amplification loop that can be inhibited by MIHA. When expressed at sufficient levels, DIABLO was able to promote caspase activation by disrupt-

Address correspondence to David L. Vaux, The Walter & Eliza Hall Institute of Medical Research, Post Office, The Royal Melbourne Hospital, Victoria 3050, Australia. Tel.: 61-3-9345-2544. Fax: 61-3-9347-0852. E-mail: vaux@wehi.edu.au

[1]*Abbreviations used in this paper:* BIR, baculoviral IAP repeat; CARD, caspase recruitment domain; IAP, inhibitor of apoptosis protein; PI, propidium iodide.

ing the interaction between MIHA and processed caspase 9, thereby leading to apoptosis.

Materials and Methods

Cell Culture and Transfection

293T cells and NT2 cells (a kind gift from D. Nicholson, Merke-Frosst, Quebec, Canada) were maintained in DME supplemented with 10% FCS. Cells were transfected using Effectene (QIAGEN) following the manufacturer's protocol. For experiments in 6-well plates (Nunc), cells were seeded at a density of 10^5 cells per well 24 h before transfection. A total of 0.2 μg DNA was used for transfections in 6-well plates along with 2.5 μl of transfection reagent. For experiments in 100-mm plates, $2–3 \times 10^6$ cells per plate were seeded 24 h before transfection, and a total of 1–2 μg of DNA was used along with 10 μl (293T cells) or 12 μl (NT2 cells) of Effectene.

Stable cell lines were made by transfecting NT2 cells with 2 μg of DNA linearized by digestion with Fsp1 (New England Biolabs, Inc.). 2 d after transfection, cells were split into four separate plates and puromycin (8 μg/ml) added to the media. Several clones from each individual plate were selected and tested for expression of protein by flow cytometry and by Western blot.

Mammalian Cell Constructs

NH_2-terminally Flag-tagged MIHA was cloned into the pEF vector (Uren et al., 1996; Huang et al., 1997). Bcl-2, LacZ, and caspase 9 were also cloned into the pEF vector but were not Flag-tagged. Untagged DIABLO was expressed in the pEF vector as described previously (Verhagen et al., 2000). Caspase 9 was cloned by PCR from an HeLa cDNA library using the following primers: 5′-CGGGGATCCCCATGGACGAAGCGGATCGGCGGC -3′ and 5′-GCTCTAGATTAGCTAGCTGATGTTTTAAAGAAAAGTTTTTTCC-3′. The PCR product was digested with BamH1 and Xba1 and subcloned into the pEF vector. The caspase recruitment domain (CARD) of caspase 9 was PCR amplified with primers 5′- CG GGA TCC ACC ATG TCC GGT GCT CTT GAG AGT TTG A-3′ and 5′-GC TCTAGA TTA GCTAGC TGA TGT TTT AAA GAA AAG TTT TTTCC-3′, cut with BamHI and XbaI, and subcloned into the pEF vector.

Yeast Constructs

Yeast vectors driving expression from either the constitutive ADH promoter or the inducible Gal1/10 promoter based on the pRS31X series of yeast vectors (Sikorski and Hieter, 1989) have been described previously (Hawkins et al., 1999, 2000; Wang et al., 1999). pGALL-(URA), was generated by swapping the PvuI fragment of pGALL-(TRP1) (Hawkins et al., 1999) containing the TRP-1 gene with that of pRS316 containing the URA selection gene. Various coding sequences were inserted into these vectors as detailed below. Plasmids expressing Apaf-$1^{1–530}$, caspase 9, and p35 have been described previously (Hawkins et al., 1999; Wang et al., 1999). The coding region of MIHA was excised from pGALL-(*HIS3*)-MIHA (Hawkins et al., 1999) and ligated into pADH-(*TRP1*). Caspase 3 was amplified from CPP32 (Fernandes et al., 1994) with oligonucleotides 1 and 2. The resulting product was digested with BamHI and XbaI and cloned into pGALL-(*URA*).

The sequences of the oligonucleotides used in these PCR reactions were: 1, CGGGATCCATGGAGAACACTGAAAACTCAGTGG; and 2, GCTCTAGATTAGTGATAAAAATAGAGTTCTTTTGTGAGC.

Yeast Transformation, Growth, and Immunoblotting

The yeast strain W303-α was used. Immunoblotting was performed as described previously (Hawkins et al., 1999; Hawkins et al., 2000) using a rabbit anti-caspase 3 antibody (BD PharMingen) at 1:2,000 and a mouse anti-caspase 9 antibody (Oncogene Research Products) at 1:200. The HRP-conjugated secondary antibodies were anti–rabbit IgG (H+L) (Pierce Chemical Co.) and anti–mouse IgG (Fab) (Sigma-Aldrich) used at 1:200,000 and 1:10,000, respectively. For enhanced chemiluminescence detection, Supersignal West Pico Substrate (Pierce Chemical Co.) was used.

Death Assays

Cells were washed twice in PBS in the tissue culture plate, and after removal of the PBS and the lid of the tissue culture plate, the cells were exposed to UV radiation in a tissue culture hood. The intensity of the UV radiation was measured using a Spectroline DM-254N ultraviolet light meter. The time required to give a certain dose (J/m^2) of UV radiation is given by the formula: time = desired dose/(μW/cm2 × 1^{e-2}). The times for the doses used were: 10 J/m^2 = 11 s, 25 J/m^2 = 26 s, 50 J/m^2 = 55 s, and 100 J/m^2 = 111 s. 6 h after UV radiation, the cells were treated with trypsin, removed from the plate, washed in DME supplemented with 10 mM $CaCl_2$, and incubated with FITC coupled or biotinylated annexin V (a kind gift from D. Huang and A. Strasser, The Walter and Eliza Hall Institute) at a dilution of 1:100 in 100 μl of DME with $CaCl_2$ and 5% FCS, for 20 min at room temperature. Cells were then washed twice and incubated with Streptavidin coupled to either Tricolor (when cells were also transfected with GFP) or phycoerythrin (Caltag) in a dilution of 1:50 in DME with $CaCl_2$ and 5% FCS for 10 min on ice. Cells were analyzed by flow cytometry.

For serum withdrawal, NT2 cells were washed three times in serum-free DME and then placed in serum-free DME. At various time points after serum withdrawal, the supernatant (which contained dead, nonadherent cells) and the remainder of the cells were removed from the plate with trypsin, washed, and incubated with 2 μg/ml propidium iodide (PI) and analyzed by flow cytometry for PI uptake.

Flow Cytometry

Analysis was done using a FACScan™ (Becton Dickinson). PI was assessed using the FL-3 channel. To determine annexin V staining of transiently transfected cells, the successfully transfected cells (GFP-positive and fluorescent in the FL-1 channel) were gated and the percentage of annexin Tricolor–positive cells was determined in the FL-3 channel. To determine the annexin staining of nontransfected cells, the Streptavidin-phycoerythin secondary agent was used and the percentage of annexin-positive cells was determined in the FL-2 channel.

Western Blots and Immunoprecipitation

Lysates were made from ~5×10^6 293T cells or NT2 cells cultured in 100-mm plates. All cells, including nonadherent cells in the supernatant, were washed twice in cold PBS and then lysed by gentle rotation in 500 μl of lysis buffer (150 mM NaCl, 10% glycerol, 1% Triton X-100, 2 mM EDTA, 1 mM PMSF, 40 mg/ml aprotinin, 20 mg/ml leupeptin) for 1 h at 4°C. The lysates were then spun at 10,000 rpm for 10 min and the supernatant was retained. These lysates were then used in Western blots or for immunoprecipitation. For Western blotting, 20–30 μl of lysate was run on a 4–20% gradient polyacrylamide gel (Gradipore) and then transferred to nitrocellulose membrane (Hybond-C; Amersham Pharmacia Biotech). After transfer, the membranes were washed in PBS and then blocked in 5% milk in PBS for 1 h and immunoblotted with primary antibody also in 5% milk. The antibodies used are listed below. As a control, agarose-coupled mouse IgG was also used to ensure protein pulled down did not nonspecifically associate with the beads (data not shown).

Anti-Flag immunoprecipitations were done by mixing 30 μl of agarose-coupled anti-Flag M2 (Sigma-Aldrich) resuspended in lysis buffer with 200 μl of lysate and the total volume was then made up to 1 ml using lysis buffer. This was gently rotated at 4°C for 1 h. The beads were pelleted by brief centrifugation and washed three times in lysis buffer. Immunoprecipitated protein was eluted by resuspending the beads in 120 μl (i.e., four times the volume of beads used) of 100 mM glycine, pH 3.0, spinning down the beads, and retaining the supernatant which was neutralized by the addition of 1:10 vol (12 μl) of Tris-HCl, pH 8.0. The immunoprecipitate was then boiled for 5 min in loading buffer and run on 4–20% gradient polyacrylamide gel (Gradipore), transferred to nitrocellulose membrane (Hybond-C; Amersham Pharmacia Biotech), and immunoblotted with the appropriate antibody.

The primary antibodies used were: anti-Flag M2 (Sigma-Aldrich), anti-caspase 3 (rabbit polyclonal; PharMingen), anti-caspase 9 (rabbit polyclonal; BD PharMingen) (designated A in Figs. 1–5), anti-caspase 9 (rabbit polyclonal; New England Biolabs, Inc.) (designated B in Figs. 1–5), anti-Smac (rabbit polyclonal; a kind gift from X. Wang, The Howard Hughes Medical Institute, University of Texas, Dallas, TX), anti-CARD caspase 9 (mouse monoclonal; a kind gift from Y. Lazebnik, Cold Spring Harbor Laboratory, Cold Spring Harbor, NY), anti-cytochrome *c* (mouse monoclonal; BD PharMingen), and anti-XIAP (mouse monoclonal; MBL [Abacus]). The secondary antibodies used were: goat anti–rabbit-HRP (Southern Biotechnology Associates, Inc.) and goat anti–mouse-HRP (Southern Biotechnology Associates, Inc.). ECL Western blotting reagents (Amersham Pharmacia Biotech) were used to detect antibody signal. All autoradiographs were scanned into Adobe Photoshop®, and the figures were made using Adobe Freehand v9.

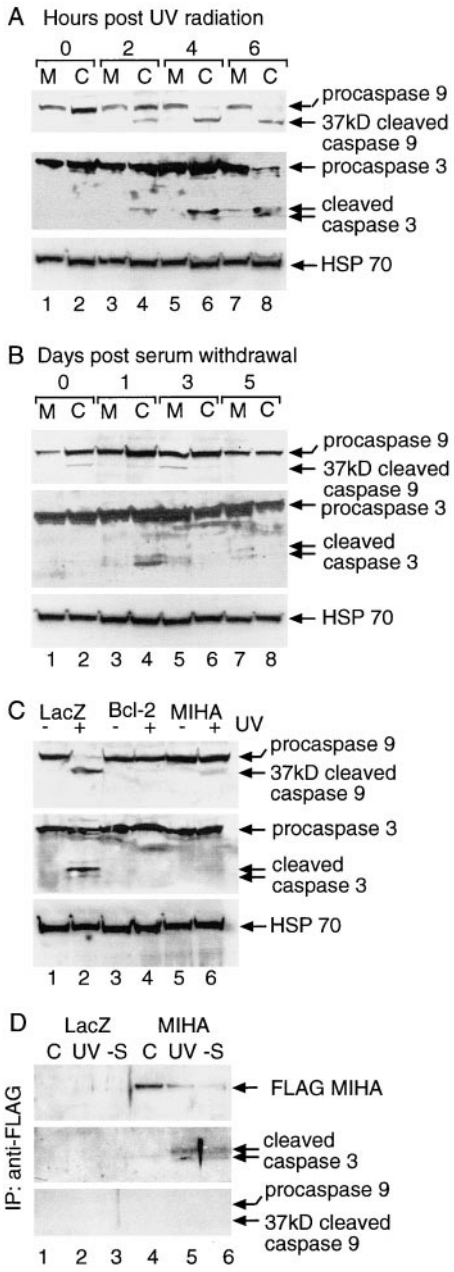

Figure 1. (A) MIHA and Bcl-2 inhibit caspase 9 and caspase 3 processing in response to UV radiation but not serum withdrawal, and MIHA binds to endogenous, processed caspase 3. NT 2 cells stably transfected with MIHA (M) or LacZ (C) were exposed to 100 J/m^2 UV radiation and lysates were harvested at 6 h. Kinetics of caspase processing was followed using Western blot immunoblotted with anti-caspase 3 and anti-caspase 9 antibodies. Full-length caspase 9 and the cleaved 37-kD fragment of caspase 9, full-length caspase 3, and the 20- and 17-kD large subunits are indicated. Almost complete processing of caspase 9 was observed in control cells, and this was inhibited by the stable expression of MIHA. Caspase 3 processing was also inhibited by MIHA, since most caspase 3 in the MIHA line remained in the unprocessed form (lane 7) compared with control cells (lane 8). (B) NT2 cells stably transfected with MIHA (M) or LacZ (C) were grown under serum-free conditions and lysates were harvested and immunoblotted with anti-caspase 3 and anti-caspase 9 antibodies. Caspase 3 cleavage occurred in both MIHA- and LacZ-expressing cells. Over the time course, most caspase 9 remained in the full-length rather than cleaved form. (C) NT2 cells stably expressing MIHA, LacZ, or Bcl-2 were exposed to 100 J/m^2 UV radiation and the lysates were harvested 24 h later and immunoblotted with anti-caspase 9 and anti-caspase 3 antibodies. MIHA lines inhibited caspase 9 and caspase 3 cleavage but not to the same degree as Bcl-2. In all the Western blots, anti-HSP70 immunoblotting was done as loading controls. (D) Flag-tagged MIHA was immunoprecipitated from the lysates of NT2 cells stably expressing MIHA or LacZ that were cultured in serum-containing media (C), or exposed to 100 J/m^2 (UV), or were cultured in serum-free media for 24 h (−S), and the immunoprecipitate was probed with anti-caspase 3 and anti-caspase 9 antibodies. Processed endogenous caspase 3 coimmunoprecipitated with MIHA after serum withdrawal and UV radiation. No association with caspase 9 in either its zymogen or processed form was detected.

Digitonin Fractionation of NT2 Cells

Digitonin fractionation of cells into cytosolic and membrane fractions was performed as described previously (Ramsby et al., 1994). In brief, NT2 cells were plated at 1.5×10^6 cells/10-cm plate and were UV irradiated (50 J/m^2) 0, 3, or 6 h before harvest. The cells were scraped off the plate and washed one time with cold PBS. The cells were then suspended in 200 μl of 0.025% digitonin (Calbiochem) in a lysis buffer (250 mM sucrose, 20 mM Hepes, pH 7.4, 5 mM $MgCl_2$, 10 mM KCl, 1 mM EDTA, 1 mM EGTA, 1 mM PMSF, 10 μg/ml aprotinin, and 10 μg/ml leupeptin). After 10 min, the cells were centrifuged (2 min, 13,000 rpm) and the supernatant was removed (cytosolic fraction). The remaining pellet was resuspended in 200 μl RIPA lysis buffer (150 mM NaCl, 1.0% NP-40, 0.5% deoxycholate, 0.1% SDS, 50 mM Tris-HCl, pH 8.0), lysis was allowed to proceed for a further 30 min, and cellular debris was removed by centrifugation. The supernatant comprising the membrane fraction was retained.

Results

MIHA Inhibits UV Radiation–induced Apoptosis, Caspase 3 and Caspase 9 Processing, but Not Serum Withdrawal–induced Apoptosis

NT2 cells stably expressing MIHA or Bcl-2 are protected from UV-induced apoptosis (Verhagen et al., 2000). However, only lines expressing Bcl-2 were able to inhibit death induced by serum starvation (data not shown). These results indicated that levels of MIHA that were sufficient to protect against apoptosis induced by UV radiation were inadequate to inhibit apoptosis induced by serum withdrawal.

To determine whether MIHA acted upstream or downstream of caspase activation, lysates from UV-treated and serum-starved cells were probed with antibodies against caspase 3 and caspase 9 (Fig. 1, A–C). In control (LacZ-transfected) cells in response to UV radiation, most caspase 9 and some caspase 3 was processed by 6 h (Fig. 1 A, lanes 2, 4, 6, and 8). In contrast, in cells expressing MIHA, cleavage of caspase 9 and caspase 3 was greatly reduced (Fig. 1 A, lanes 1, 3, 5, and 7). By 24 h after UV treatment (Fig. 1 C), cleavage of caspase 9 but not caspase 3 was observed in MIHA-expressing cells (Fig. 1 C, lanes 5 and 6), whereas cells expressing Bcl-2, which were used as a positive control for protection against UV radiation–induced apoptosis, showed minimal processing of caspase 9 and caspase 3 (Fig. 1 C, lanes 3 and 4). Control cell lines showed almost complete cleavage of caspase 9 and partial cleavage of caspase 3 (Fig. 1 C, lanes 1 and 2). These results suggest that both Bcl-2 and MIHA inhibit UV-induced apoptosis at a point before caspase 9 and caspase

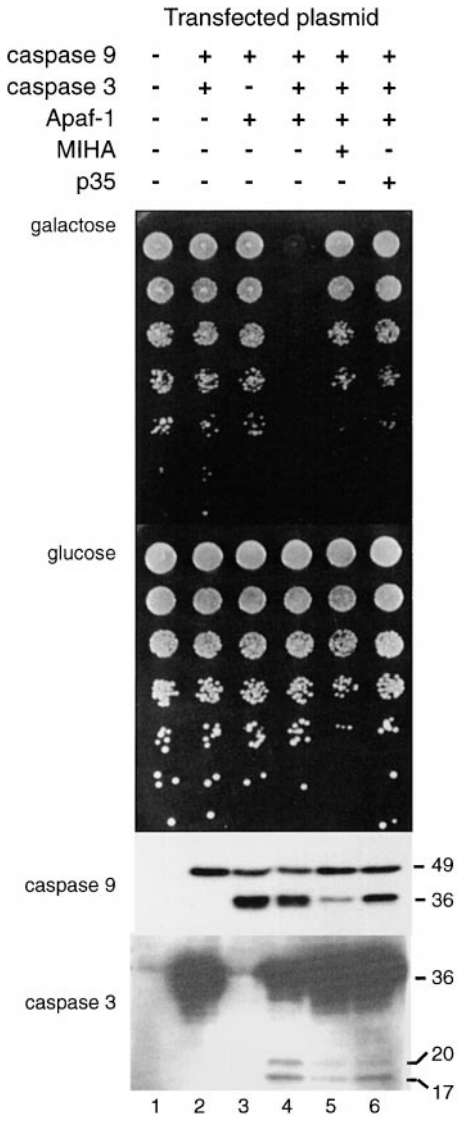

Figure 2. Expressing a truncated form of Apaf-1, procaspase 9 and procaspase 3 in *S. cerevisiae* can kill yeast, and this can be inhibited by MIHA. *S. cerevisiae* clones expressing the constructs indicated at the top were grown under inducing (galactose) or noninducing (glucose) conditions. Transformants expressing truncated Apaf-1, procaspase 9, and procaspase 3 were killed (galactose, lane 4) unless protected by either MIHA or p35 (lanes 5 and 6). The same transformants were induced in liquid medium for 8 h, and lysates were immunoblotted with anti-caspase 9 and anti-caspase 3 antibodies (bottom two panels). Apaf-$1^{1–530}$ caused processing of caspase 9 but did not kill yeast (lane 3). Procaspase 3 was cleaved by processed caspase 9 (lane 4), which resulted in death of the yeast. Both caspase 3 and caspase 9 processing was inhibited by MIHA and to a lesser degree, p35.

3 are fully processed, although MIHA incompletely inhibits caspase 9 processing.

Analysis of caspase activation in the serum-starved cells (Fig. 1, B and C) revealed that little caspase 9 processing occurred in any of the lines, with most remaining as the 50-kD proform. Caspase 3 cleavage did occur and was not inhibited by MIHA (Fig. 1 C, lanes 3–8). These experiments suggest that caspase 9 does not play a significant role in serum withdrawal–induced apoptosis. Because MIHA could prevent caspase 3 activation after UV irradiation, but not after serum starvation, these results also imply that caspase 3 activation occurs by different pathways after each apoptotic stimulus.

MIHA Binds to Endogenous, Processed Caspase 3 but Not Procaspase 9

To determine whether MIHA acts on caspases directly, we performed coimmunoprecipitations from lysates obtained from the same NT2 lines used to demonstrate caspase cleavage in response to UV radiation and serum withdrawal (Fig. 1 D). Although both the zymogen and processed forms of caspase 3 were present in the lysates, MIHA only coimmunoprecipitated the processed form of caspase 3 (Fig. 1 D, lanes 3 and 4). MIHA did not coimmunoprecipitate any procaspase 9. These data suggest that MIHA is able to bind to processed caspase 3 but not to the zymogen forms of either caspase 3 or caspase 9.

Caspase 9 Processes Caspase 3 in Saccharomyces cerevisiae and MIHA Can Inhibit both Caspase 9 and Caspase 3 Processing

Yeast offers a convenient system in which to test mammalian components of the apoptosis mechanism because yeast do not encode caspases or their inhibitors. To test the function of MIHA in a yeast system, a truncated, constitutively active Apaf-1 (Apaf-$1^{1–530}$), procaspase 9, and procaspase 3 were expressed in *S. cerevisiae*, and the effects of MIHA on viability and caspase activation were examined. Although autoactivating caspase 3, or caspase 3 processed by an autoactivating caspase 9, kills *S. cerevisiae* (Kang et al., 1999; Wright et al., 1999) caspase 9 alone, or caspase 9 coexpressed with Apaf-$1^{1–530}$, was not toxic, even though in the latter situation, caspase 9 processing occurred (Fig. 2, lanes 2 and 3). When wild-type caspase 3 was coexpressed with procaspase 9 and Apaf-1, yeast growth was strongly inhibited, and both caspase 9 and caspase 3 processing occurred (Fig. 2, lane 4). In contrast, wild-type procaspase 9 did not autoprocess or inhibit yeast growth in the absence of Apaf-1, even when coexpressed with procaspase 3 (Fig. 2, lane 2). These results show that activation of caspase 9 by Apaf-1 and subsequent activation of caspase 3 can be recapitulated in *S. cerevisiae*. Processing of caspase 9 alone was insufficient to cause death of the yeast, which required the further activation of caspase 3 by caspase 9.

To determine where MIHA acts to prevent caspase 3–mediated yeast cell death, we coexpressed MIHA along with the caspases and Apaf-$1^{1–530}$ (Fig. 2, lanes 5 and 6). MIHA was able to rescue the yeast as efficiently as the baculoviral caspase inhibitor, p35. Processing of both caspase 9 and caspase 3 was diminished in the presence of MIHA. These data show that MIHA can inhibit the processing of both caspase 3 and caspase 9. Because the processing of caspase 3 in this system is caspase 9 dependent, MIHA appears to inhibit active caspase 9 directly, thus preventing it from cleaving procaspase 3. MIHA may prevent cleavage of caspase 9 either directly by binding to activated caspase 3, or indirectly by reducing the amount of caspase 3 that becomes activated.

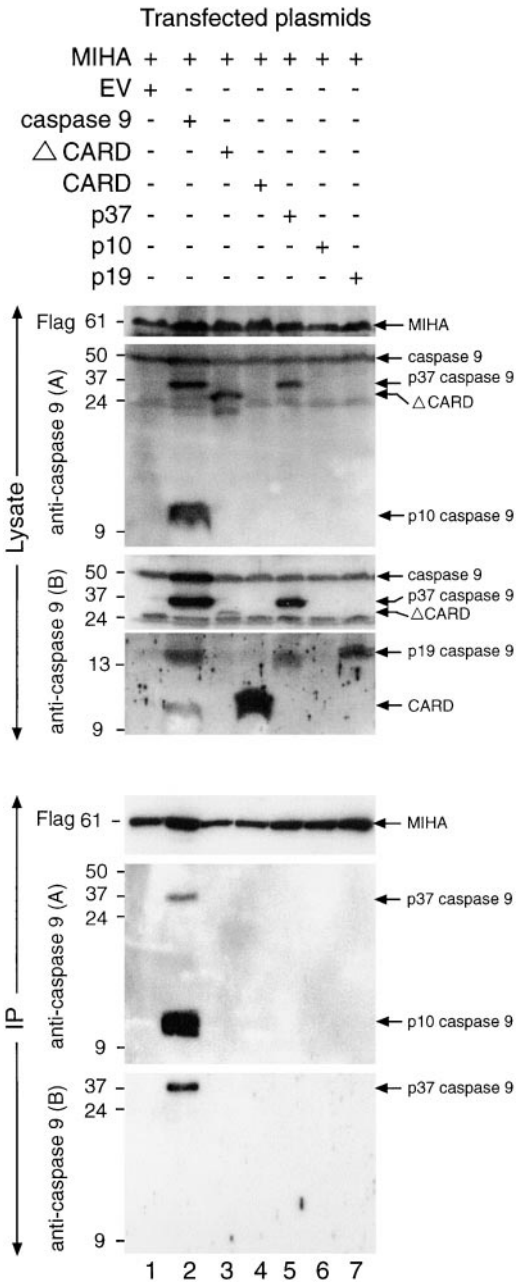

Figure 3. MIHA binds to processed, active caspase 9 and not to the zymogen form of caspase 9. 293T cells were transfected with Flag-tagged MIHA and the indicated constructs (EV, empty vector; ΔCARD, caspase 9 lacking the prodomain; CARD, prodomain only; p37, prodomain and large subunit; p10, small subunit only; p19, large subunit only). MIHA was immunoprecipitated and the lysates and immunoprecipitate (IP) were probed with the antibodies indicated on the left. Two caspase 9 antibodies were used: A, which recognizes the p10 and ΔCARD as well as full-length caspase 9 and the p37; and B, which recognizes the CARD and the p19 as well as the p37 fragment of caspase 9 and full-length caspase 9. FL, anti-Flag antibody. MIHA coimmunoprecipitated the processed (37-kD) and p10 subunit of caspase 9 (lane 2) but only when caspase 9 was transfected as a full-length construct and underwent processing within the cell (lane 2). None of the individual components of caspase 9 immunoprecipitated with MIHA, suggesting that MIHA binds only to the processed enzyme in its active conformation.

MIHA Binds to Processed Caspase 9 and Functions Downstream of Mitochondrial Cytochrome c and DIABLO Release

To determine if MIHA could bind to caspase 9, 293T cells were transiently transfected with MIHA and procaspase 9. Full-length caspase 9 underwent autoprocessing under these transfection conditions (Fig. 3, lane 2). When both full-length and processed caspase 9 were present, MIHA only bound to the processed, active form of caspase 9 (Fig. 3, lane 2). MIHA could not immunoprecipitate endogenous procaspase 9 (Fig. 3, lane 1). When constructs encoding the various subunits of caspase 9 were independently transfected along with MIHA (Fig. 3, lanes 3–7), none were able to bind to MIHA, including constructs encoding the CARD and the large subunit (Fig. 3, lane 5) and the small subunit (Fig. 3, lane 6), both of which bound to MIHA when full-length caspase 9 was cotransfected. A construct lacking the CARD (ΔCARD) (Hofmann et al., 1997) also did not bind to MIHA (Fig. 3, lane 3). These results suggest that MIHA bound only to processed caspase 9 in its active configuration since MIHA bound caspase 9 only when the full-length enzyme was transfected, immunoprecipitating the processed subunits of the enzyme (the p37 and p10). None of the individual subunits of caspase 9 were capable of binding to MIHA independently.

Because MIHA appears to associate preferentially with processed caspase 9, this suggests that MIHA functions downstream of caspase 9 cleavage. We have shown previously that MIHA does not prevent the mitochondrial release of cytochrome *c* or DIABLO in response to UV radiation (Verhagen et al., 2000). To investigate this further, we analyzed membrane and cytosolic fractions of UV-treated NT2 cells stably transfected with MIHA, Bcl-2, or LacZ (Fig. 4). In control (LacZ) cells (Fig. 4, lanes 1–6) and MIHA-expressing cells (Fig. 4, lanes 13–18), DIABLO and cytochrome *c* were detectable in the cytosolic fractions 3 h after UV radiation. Caspase 9 and caspase 3 were present almost exclusively in the cytosolic fractions and were processed in control cells after UV radiation. In cells expressing Bcl-2 (Fig. 4, lanes 7–12) or MIHA, processing of caspase 9 and caspase 3 in response to UV radiation was prevented. These data suggest that MIHA functions downstream of cytochrome *c* and DIABLO release from mitochondria to prevent full activation of caspase 9, whereas Bcl-2 acts upstream of the mitochondrial events. Together with the results showing the effect of MIHA on caspase cleavage in response to UV radiation, this suggests that in mammalian cells, as in the yeast system, MIHA functions primarily to prevent the activation of caspase 3 by active caspase 9 and can also prevent the feedback cleavage of caspase 9.

DIABLO Disrupts MIHA Binding to Processed Caspase 9

DIABLO can antagonize the antiapoptotic functions of MIHA (Du et al., 2000; Verhagen et al., 2000). To determine how it does so, 293T cells were transfected with caspase 9 and varying ratios of DIABLO and MIHA (Fig. 5). MIHA coimmunoprecipitated processed caspase 9 in the absence of transfected DIABLO or when the MIHA/DIABLO ratio was 4:1 (lanes 1–2). At ratios less than

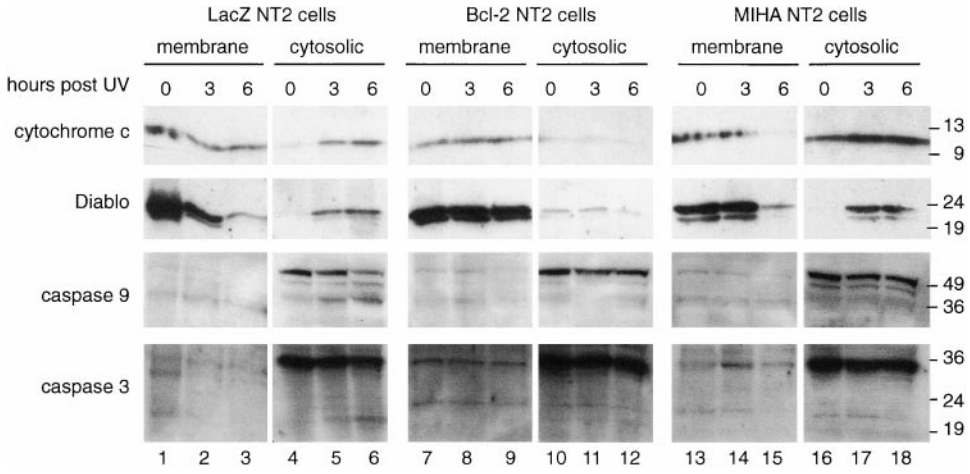

Figure 4. MIHA acts downstream of mitochondrial cytochrome *c* and DIABLO release. NT2 cells stably transfected with LacZ, Bcl-2, or MIHA were exposed to UV radiation for the indicated times. The cells were harvested and membrane and cytosolic fractions were separated. The two fractions were then immunoblotted with anti-caspase 3, anti-caspase 9, anti-cytochrome *c* and anti-DIABLO antibodies. Control (LacZ) cells show translocation of cytochrome *c* and DIABLO to the cytosolic fraction and cleavage of cytosolic caspase 3 and caspase 9 (lanes 1–6). All these processes were inhibited in cells expressing Bcl-2 (lanes 7–12). MIHA inhibited processing of caspase 9 and caspase 3, but cytochrome *c* and DIABLO translocated from membrane to cytosolic fractions to the same degree as in control cells (lanes 13–18).

this, DIABLO was able to prevent the binding of MIHA to processed caspase 9, even though similar amounts of caspase 9 and MIHA were present (lanes 3–5). These data show that DIABLO counters the antiapoptotic action of MIHA by preventing MIHA from associating with active caspase 9.

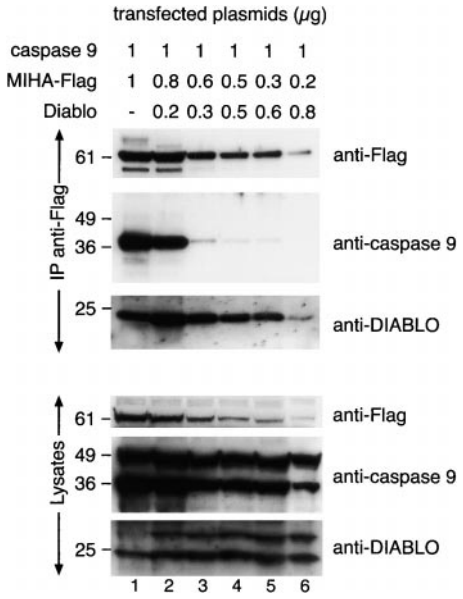

Figure 5. DIABLO inhibits the binding of processed caspase 9 to MIHA. 293T cells were transfected as indicated. 48 h after transfection, the lysates were harvested and MIHA was immunoprecipitated. Both the lysates and the immunoprecipitates (IP, indicated on the left) were immunoblotted with anti-caspase 9, anti-DIABLO, and anti-Flag antibody. MIHA coimmunoprecipitated processed, but not full-length, caspase 9 (lane 1). This association persisted when the MIHA/DIABLO ratio was 4:1 (lane 2) but was significantly inhibited by DIABLO at lower ratios (lanes 3–6). Endogenous and transfected DIABLO were able to associate with MIHA. The full-length (50-kD) and processed forms (37-kD) of caspase 9 were present in the lysates. Transfected DIABLO was expressed in both an unprocessed (25-kD) and processed (23-kD) form. The processed form coimmunoprecipitated with MIHA.

Discussion

The antiapoptotic activity of a subgroup of mammalian IAPs (MIHA/XIAP, MIHB/cIAP1, and MIHC/cIAP2) has been ascribed principally to the ability of these proteins to directly inhibit both active caspases and caspase activation. XIAP, cIAP1, and cIAP2 have been shown to bind to activated caspase 3 and procaspase 9 (Deveraux et al., 1997, 1998; Takahashi et al., 1998). We have shown that MIHA, the murine homologue of XIAP (Uren et al., 1996), is able to inhibit caspase 9 and caspase 3 activation in response to UV radiation and that MIHA can associate with endogenous, processed caspases 3 and transfected caspase 9. We were not able to demonstrate any binding of MIHA with procaspase 3 or procaspase 9, either in response to a death stimulus (serum withdrawal or UV radiation) or in a transient transfection assay.

The binding of MIHA to processed caspase 3 did not appear to be sufficient for MIHA to inhibit apoptosis. We observed association between MIHA and processed caspase 3 under conditions in which caspase 3 became activated, including serum withdrawal where caspase 3 activation appeared independent of caspase 9 activation and when the cells were ultimately to die. However, when apoptosis was induced by UV radiation, a death stimulus in which caspase 9 was processed and in which caspase 9 has been shown to play a critical role (Hakem et al., 1998), MIHA was able to inhibit apoptosis. These results suggest that while MIHA can bind to and inhibit both processed caspase 3 and caspase 9, the interaction with caspase 9 is more critical for the inhibition of apoptosis.

The prodomain of caspase 9 contains a CARD that mediates binding between caspase 9 and Apaf-1 (Day et al., 1999; Qin et al., 1999). MIHA was able to bind to the processed, active form of caspase 9 (containing the CARD) but not to the individual subunits of caspase 9 when transfected independently. MIHA coimmunoprecipitated with the CARD and large subunit (p37) and the small subunit (p10) when these were generated by autoprocessing of the proenzyme. This strongly suggests that MIHA binds to the processed, active heterotetrameric form of caspase 9 rather than the zymogen form of the enzyme as has been

reported previously (Deveraux et al., 1998). One possible reason for this discrepancy with previously published results is that in our system, both inactive and active caspase 9 are available for binding, allowing MIHA to demonstrate a preference for binding to the active form of the enzyme. In other systems, only the zymogen form of the enzyme was available for binding. Another explanation is that MIHA is able to bind initially to the zymogen form of caspase 9, but is unable to prevent subsequent caspase 9 processing within the apoptosome. Our data do not define the interacting domains of caspase 9 or MIHA. Thus, MIHA may act like the *Drosophila* IAP, DIAP1, which can bind to the caspase DRONC via its CARD (Meier et al., 2000), although other evidence suggests that XIAP can bind to caspase 9 (lacking a CARD) via its BIR3 (Sun et al., 2000).

In mammalian cells and in yeast, our data show that caspase 9 processes caspase 3 and this can be inhibited by MIHA. The partial inhibition of caspase 9 processing by MIHA suggests either that MIHA can inhibit autocatalytic activation of caspase 9, or that it can inhibit processing of caspase 9 by caspase 3 in an amplification loop. Such an amplification loop is consistent with the ability of MIHA to bind to endogenous processed caspase 3 and the ability of caspase 3 to cleave and activate caspase 9 (Deveraux et al., 1998; Woo et al., 1999). Furthermore, experiments in caspase 9–deficient mice show that in some death pathways, caspase 3 cleavage is caspase 9 dependent (Hakem et al., 1998; Kuida et al., 1998). MIHA functions by binding to the active forms of these caspases and preventing the amplification loop from proceeding. This explains the apparent paradox that although MIHA binds to processed caspases, it is nevertheless able to reduce the amount of caspase cleavage.

Once released from mitochondria, DIABLO functions to prevent MIHA from binding to processed caspase 9 and thereby stops MIHA from blocking the amplification of caspase activation. Whereas high levels of DIABLO can efficiently neutralize MIHA, DIABLO cannot antagonize the antiapoptotic effect of Bcl-2, not only because Bcl-2 prevents DIABLO release from mitochondria, but also because it can block signals that lead to caspase 9 activation (Verhagen et al., 2000).

We thank Drs. D.C.S. Huang and A. Strasser for advice and reagents, X.D. Wang for the anti-Smac antibody, Y. Lazebnik for the anti-CARD antibody, and D. Nicholson for wild-type NT2 cells.

This work was supported by a National Health and Medical Research Council (Australia) grant to Walter and Eliza Hall Institute (RegKey 973002). P.G. Ekert is supported by a postdoctoral fellowship from the Murdoch Children's Research Institute. A. Verhagen is a recipient of a C.J. Martin Scholarship from the National Health and Medical Research Council. D.L. Vaux is a scholar of the Leukemia and Lymphoma Society.

Submitted: 28 August 2000
Revised: 19 December 2000
Accepted: 20 December 2000

References

Claveria, C., J.P. Albar, A. Serrano, J.M. Buesa, J.L. Barbero, A.C. Martinez, and M. Torres. 1998. *Drosophila* grim induces apoptosis in mammalian cells. *EMBO (Eur. Mol. Biol. Organ.) J.* 17:7199–7208.

Clem, R.J., and L.K. Miller. 1994. Control of programmed cell death by the baculovirus genes p35 and IAP. *Mol. Cell. Biol.* 14:5212–5222.

Crook, N.E., R.J. Clem, and L.K. Miller. 1993. An apoptosis inhibiting baculovirus gene with a zinc finger like motif. *J. Virol.* 67:2168–2174.

Day, C.L., C. Dupont, M. Lackmann, D.L. Vaux, and M.G. Hinds. 1999. Solution structure and mutagenesis of the caspase recruitment domain (CARD) from Apaf-1. *Cell Death Differ.* 6:1125–1132.

Deveraux, Q.L., R. Takahashi, G.S. Salvesen, and J.C. Reed. 1997. X-linked IAP is a direct inhibitor of cell-death proteases. *Nature*. 388:300–304.

Deveraux, Q.L., N. Roy, H.R. Stennicke, T. Vanarsdale, Q. Zhou, S.M. Srinivasula, E.S. Alnemri, G.S. Salvesen, and J.C. Reed. 1998. IAPs block apoptotic events induced by caspase-8 and cytochrome *c* by direct inhibition of distinct caspases. *EMBO (Eur. Mol. Biol. Organ.) J.* 17:2215–2223.

Deveraux, Q.L., E. Leo, H.R. Stennicke, K. Welsh, G.S. Salvesen, and J.C. Reed. 1999. Cleavage of human inhibitor of apoptosis protein XIAP results in fragments with distinct specificities for caspases. *EMBO (Eur. Mol. Biol. Organ.) J.* 18:5242–5251.

Du, C., M. Fang, Y. Li, L. Li, and X. Wang. 2000. Smac, a mitochondrial protein that promotes cytochrome *c*–dependent caspase activation by eliminating IAP inhibition. *Cell*. 102:33–42.

Duckett, C.S., V.E. Nava, R.W. Gedrich, R.J. Clem, J.L. Vandongen, M.C. Gilfillan, H. Shiels, J.M. Hardwick, and C.B. Thompson. 1996. A conserved family of cellular genes related to the baculovirus IAP gene and encoding apoptosis inhibitors. *EMBO (Eur. Mol. Biol. Organ.) J.* 15:2685–2694.

Fernandes, A.T., G. Litwack, and E.S. Alnemri. 1994. CPP32, a novel human apoptotic protein with homology to *Caenorhabditis elegans* cell death protein CED-3 and mammalian interleukin-1 beta-converting enzyme. *J. Biol. Chem.* 269:30761–30764.

Goyal, L., K. McCall, J. Agapite, E. Hartwieg, and H. Steller. 2000. Induction of apoptosis by *Drosophila* reaper, hid, and grim through inhibition of IAP function. *EMBO (Eur. Mol. Biol. Organ.) J.* 19:589–597.

Haining, W.N., C. Carboy-Newcomb, C.L. Wei, and H. Steller. 1999. The proapoptotic function of *Drosophila* Hid is conserved in mammalian cells. *Proc. Natl. Acad. Sci. USA*. 96:4936–4941.

Hakem, R., A. Hakem, G.S. Duncan, J.T. Henderson, M. Woo, M.S. Soengas, A. Elia, J.L. Delapompa, D. Kagi, W. Khoo, et al. 1998. Differential requirement for caspase 9 in apoptotic pathways in vivo. *Cell*. 94:339–352.

Hawkins, C.J., S.L. Wang, and B.A. Hay. 1999. A cloning method to identify caspases and their regulators in yeast: identification of *Drosophila* IAP1 as an inhibitor of the *Drosophila* caspase DCP-1. *Proc. Natl. Acad. Sci. USA*. 96:2885–2890.

Hawkins, C.J., S.J. Yoo, E.P. Peterson, S.L. Wang, S.Y. Vernooy, and B.A. Hay. 2000. The *Drosophila* caspase DRONC cleaves following glutamate or aspartate and is regulated by DIAP1, HID, and GRIM. *J. Biol. Chem.* 275: 27084–27093.

Hay, B.A., D.A. Wassarman, and G.M. Rubin. 1995. *Drosophila* homologs of baculovirus inhibitor of apoptosis proteins function to block cell death. *Cell*. 83:1253–1262.

Hofmann, K., P. Bucher, and J. Tschopp. 1997. The CARD domain—a new apoptotic signaling motif. *Trends Biochem. Sci.* 22:155–156.

Huang, D., S. Cory, and A. Strasser. 1997. Bcl-2, Bcl-x(l) and adenovirus protein E1B19kD are functionally equivalent in their ability to inhibit cell death. *Oncogene*. 14:405–414.

Kaiser, W.J., D. Vucic, and L.K. Miller. 1998. The *Drosophila* inhibitor of apoptosis D-IAP1 suppresses cell death induced by the caspase drICE. *FEBS Lett.* 440:243–248.

Kang, J.J., M.D. Schaber, S.M. Srinivasula, E.S. Alnemri, G. Litwack, D.J. Hall, and M.A. Bjornsti. 1999. Cascades of mammalian caspase activation in the yeast *Saccharomyces cerevisiae*. *J. Biol. Chem.* 274:3189–3198.

Kuida, K., T.F. Haydar, C.Y. Kuan, Y. Gu, C. Taya, H. Karasuyama, M. Su, P. Rakic, and R.A. Flavell. 1998. Reduced apoptosis and cytochrome *c*-mediated caspase activation in mice lacking caspase 9. *Cell*. 94:325–337.

LaCasse, E.C., S. Baird, R.G. Korneluk, and A.E. MacKenzie. 1998. The inhibitors of apoptosis (IAPs) and their emerging role in cancer. *Oncogene*. 17: 3247–3259.

Liston, P., N. Roy, K. Tamai, C. Lefebvre, S. Baird, G. Chertonhorvat, R. Farahani, M. Mclean, J.E. Ikeda, A. Mackenzie, and R.G. Korneluk. 1996. Suppression of apoptosis in mammalian cells by NAIP and a related family of IAP genes. *Nature*. 379:349–353.

McCarthy, J.V., and V.M. Dixit. 1998. Apoptosis induced by *Drosophila* reaper and grim in a human system—attenuation by inhibitor of apoptosis proteins (cIAPs). *J. Biol. Chem.* 273:24009–24015.

Meier, P., J. Silke, S.J. Leevers, and G.I. Evan. 2000. The *Drosophila* caspase DRONC is regulated by DIAP1. *EMBO (Eur. Mol. Biol. Organ.) J.* 19:598–611.

Qin, H., S.M. Srinivasula, G. Wu, T. Fernandes-Alnemri, E.S. Alnemri, and Y. Shi. 1999. Structural basis of procaspase-9 recruitment by the apoptotic protease-activating factor 1. *Nature*. 399:549–557.

Ramsby, M.L., G.S. Makowski, and E.A. Khairallah. 1994. Differential detergent fractionation of isolated hepatocytes: biochemical, immunochemical and two-dimensional gel electrophoresis characterization of cytoskeletal and noncytoskeletal compartments. *Electrophoresis*. 15:265–277.

Roy, N., Q.L. Deveraux, R. Takahashi, G.S. Salvesen, and J.C. Reed. 1997. The c-IAP-1 and c-IAP-2 proteins are direct inhibitors of specific caspases. *EMBO (Eur. Mol. Biol. Organ.) J.* 16:6914–6925.

Sikorski, R.S., and P. Hieter. 1989. A system of shuttle vectors and yeast host strains designed for efficient manipulation of DNA in *Saccharomyces cerevi-*

siae. *Genetics*. 122:19–27.

Song, Z.W., B. Guan, A. Bergman, D.W. Nicholson, N.A. Thornberry, E.P. Peterson, and H. Steller. 2000. Biochemical and genetic interactions between *Drosophila* caspases and the proapoptotic genes rpr, hid, and grim. *Mol. Cell. Biol*. 20:2907–2914.

Sun, C., M. Cai, R.P. Meadows, N. Xu, A.H. Gunasekera, J. Herrmann, J.C. Wu, and S.W. Fesik. 2000. NMR structure and mutagenesis of the third bir domain of the inhibitor of apoptosis protein XIAP. *J. Biol. Chem.* 275: 33777–33781.

Takahashi, R., Q. Deveraux, I. Tamm, K. Welsh, N. Assamunt, G.S. Salvesen, and J.C. Reed. 1998. A single BIR domain of XIAP sufficient for inhibiting caspases. *J. Biol. Chem*. 273:7787–7790.

Uren, A.G., M. Pakusch, C.J. Hawkins, K.L. Puls, and D.L. Vaux. 1996. Cloning and expression of apoptosis inhibitory protein homologs that function to inhibit apoptosis and/or bind tumor necrosis factor receptor-associated factors. *Proc. Natl. Acad. Sci. USA*. 93:4974–4978.

Uren, A.G., E.J. Coulson, and D.L. Vaux. 1998. Conservation of baculovirus inhibitor of apoptosis repeat proteins (BIRps) in viruses, nematodes, vertebrates and yeasts. *Trends Biochem. Sci*. 23:159–162.

Verhagen, A., P.G. Ekert, J. Silke, L.M. Connolly, G.E. Reid, R.L. Moritz, R.J. Simpson, and D.L. Vaux. 2000. Identification of DIABLO, a mammalian protein that promotes apoptosis by binding to and antagonizing IAP proteins. *Cell*. 102:43–53.

Vucic, D., W.J. Kaiser, A.J. Harvey, and L.K. Miller. 1997. Inhibition of reaper-induced apoptosis by interaction with inhibitor of apoptosis proteins (IAPs). *Proc. Natl. Acad. Sci. USA*. 94:10183–10188.

Vucic, D., W.J. Kaiser, and L.K. Miller. 1998. Inhibitor of apoptosis proteins physically interact with and block apoptosis induced by *Drosophila* proteins HID and GRIM. *Mol. Cell. Biol*. 18:3300–3309.

Wang, S.L., C.J. Hawkins, S.J. Yoo, H.-A.J. Müller, and B.A. Hay. 1999. The *Drosophila* caspase inhibitor DIAP1 is essential for cell survival and is negatively regulated by HID. *Cell*. 98:453–463.

Woo, M., A. Hakem, A.J. Elia, R. Hakem, G.S. Duncan, B.J. Patterson, and T.W. Mak. 1999. In vivo evidence that caspase-3 is required for Fas-mediated apoptosis of hepatocytes. *J. Immunol*. 163:4909–4916.

Wright, M.E., D.K. Han, L. Carter, S. Fields, S.M. Schwartz, and D.M. Hockenbery. 1999. Caspase-3 inhibits growth in *Saccharomyces cerevisiae* without causing cell death. *FEBS Lett*. 446:9–14.